Exploration of two layer Nb_3Sn designs of the Future Circular Collider Main Quadrupoles

C. Lorin, J. Fleiter, T. Salmi, D. Schoerling

***Abstract*— The goal of the present study is to propose an alternative FCC quadrupole design where the risk from both their fabrication and their operation in the machine is reduced compared to previous analysis. Therefore, the number of coil layers has been reduced from four to two layers and the load-line margin increased from 14% to 20% compared to previous investigations [1]. Indeed, the idea is to only challenge the ~5000 FCC main dipoles and stay at a relatively low complexity for the ~700 FCC main quadrupoles so they have a limiting impact on the machine operation and reliability. An exploration of the strand diameter (0.7 mm to 0.9 mm), cable size (40 to 60 strands) as well as protection delay (30 ms to 40 ms) is performed on 2D magnetic designs of the FCC main quadrupole. A discussion on cable windability allows for the selection of one design generating 367 T/m. The design is mechanically constrained with a conventional collar structure leading to collaring peak stress of 115 MPa. A single coupling loss induced quench unit ensure a safe magnet operation with a 300 K hotspot temperature.**

***Index Terms*—Nb_3Sn coil, collar structure, CLIQ protection system, MQ**

I. Introduction

In the frame of a collaboration agreement between CERN and CEA, the Main Quadrupole (MQ) design of the so-called Future Circular Collider (FCC) is investigated. The present work is included in the magnet section of the FCC Conceptual Design Report. It is worth reminding that the initial philosophy was to push the MQ to their gradient limit in order to reduce their length and give some extra length to the FCC main dipoles (MB) inside the FODO cell [2]. Each FCC FODO cell consists in 2 quadrupoles and 12 dipoles. Such approach was based on a reduction of the quantity of Nb_3Sn conductor for the whole machine considering both the MB and MQ. After a detailed study of a 4-layer design, it seems more risky to build challenging 4-layer quadrupoles besides the also challenging and more numerous 4-layers dipoles. Therefore, the complexity of the MQ assembly is mitigated by setting a 2-layer configuration as the baseline. Similarly to the LHC at nominal (7 TeV per beam), the load-line margin is increased to 20% with respect to 14% for the MB. These two measures are taken with the aim to minimize the impact of the MQ training on the operation of the FCC machine. Based on this philosophy and after some iterations with the FCC beam opticians and the FCC main dipole designers it was decided to set the integrated gradient of the FCC MQ to 2592 T with a nominal gradient of 360 T/m.

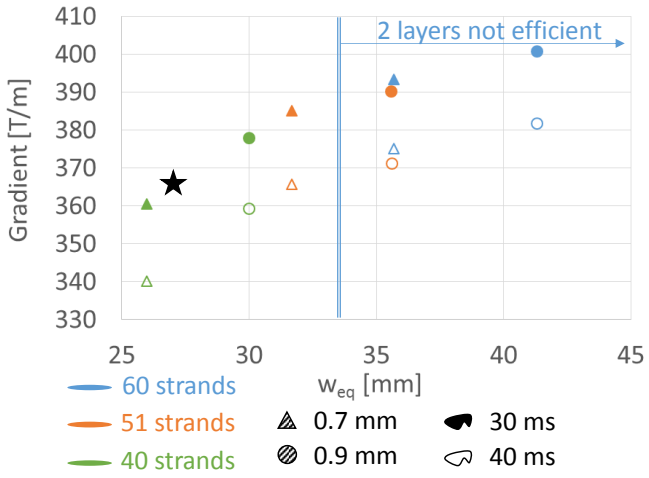

Fig. 1. Parametric analysis of the gradient versus the coil size for various cable strand diameter, number of strands in the cable and protection delays. The star represents the design (v12) described in section III of the paper.

II. 2D Parametric Exploration

A. Parameters space

First, the critical current density J_c of the Nb_3Sn conductor is the FCC target density (J_c = 2300 A/mm² @ 1.9 K and 16 T) with a 3% cabling degradation.

$$\begin{cases} J_c = \dfrac{C(t)}{B} b^{0.5}(1-b)^2 \\ B_{c2}(T) = B_{c20}(1-t^{1.52}) \\ C(t) = C_0(1-t^{1.52})^{\alpha}(1-t^2)^{\alpha} \end{cases}$$

where $t = T/T_{c0}$ and $b = B/B_{c2}(t)$ and B is the magnetic flux density on the conductors. T_{c0} = 16 K, B_{c20} = 29.38 T, α = 0.96, C_0 = 275880 AT/mm² are fitting parameters [6]-[8].

Manuscript receipt and acceptance dates will be inserted here. Acknowledgment of support is placed in this paragraph as well. *(Corresponding author: Clement Lorin.)*

C. Lorin is with CEA, 91191 Gif-sur-Yvette, France (e-mail: clement.lorin@cea.fr).

J. Fleiter and D. Schoerling are with CERN, 1211 Geneve, Switzerland.

T. Salmi is with Tampere University of Technology, 33720 Tampere, Finland.

Color versions of one or more of the figures in this paper are available online at http://ieeexplore.ieee.org.

Digital Object Identifier will be inserted here upon acceptance.

The impact on the gradient of three parameters is explored:

- The strand diameter: 0.7 mm and 0.9 mm;
- The number of cable strands: 40, 51 and 60;
- The total protection delay: 30 ms and 40 ms.

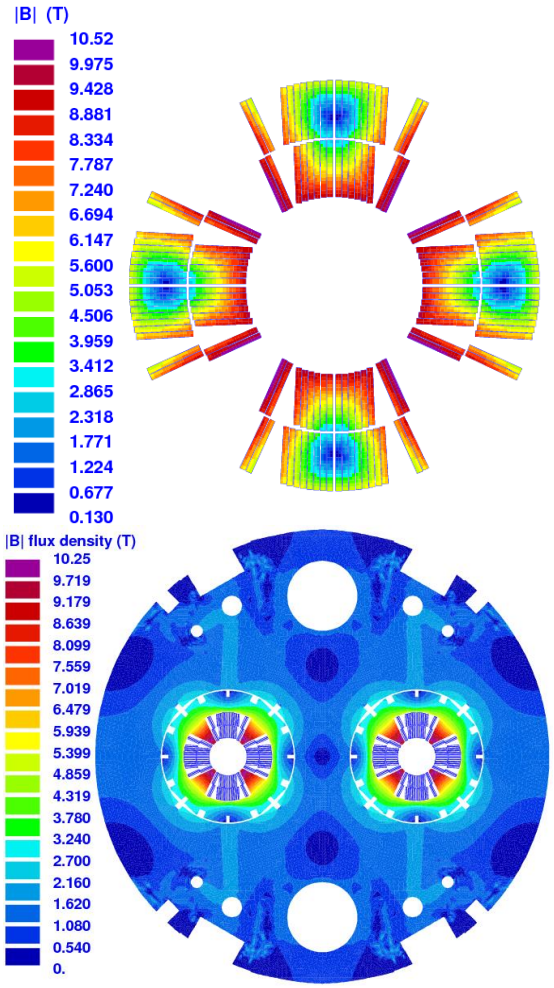

Fig. 2. Flux density distribution in the FCC MQ magnet. Top: coil cross-section (ROXIE sofware). Bottom: collars and yoke.

TABLE I
FCC MQ CABLE CHARACTERISTICS

Parameters	Units	FCC MQ (v12)
Strand diameter	mm	0.85
Cu/nonCu	-	1.65
Number of strands	-	35
Bare width (before/after HT)	mm	15.956/16.120
Bare thickness(before/after HT)	mm	1.493/1.538
Bare thin edge (before/after HT)	mm	1.438/1.481
Bare thick edge (before/after HT)	mm	1.549/1.596
Cable width expansion	%	1
Cable thickness expansion	%	3
Keystone angle	°	0.4
Transposition pitch length	mm	96
Insulation thickness per side at 5 MPa	mm	0.15

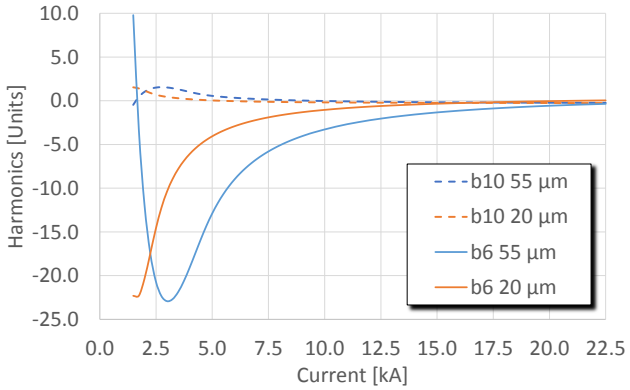

Fig. 3. Combined geometric, saturation and persistent current errors on the first two allowed multipoles b_6 and b_{10} from injection at 3.3 TeV/beam to nominal at 50 TeV/beam with 2 different filament sizes (55 µm: MQXF strand state of the art; 20 µm: FCC target).

TABLE II
FCC MQ MAGNET CHARACTERISTICS

Parameters	Units	FCC MQ (v12)
Gradient	T/m	367
Current	A	22500
Peak field	T	10.52
Load-line margin	%	20.1
Temperature margin	K	4.6
Inductance (2 apertures)	mH/m	2.04
Stored energy (2 apertures)	kJ/m	520
Azimuthal force per ½ coil	MN/m	1.74
Radial force per ½ coil	MN/m	0.4
Midplane shim	µm	325
Interlayer insulation	mm	0.5
Number of turns per layer	-	8 + 10
Area of conductor per magnet	cm²	57.2
Estimated weight of conductor*	tonnes	270

*Weight estimated for the 744 MQs of the FCC with a conductor density

The protection delay is the time from the quench ignition till the whole coil is resistive. A delay of 40 ms tends to represent conventional quench heater technology whereas the 30 ms delay is more representative of a CLIQ system [9]. A detailed protection analysis is discussed in the coming sections.

B. Results

Each dot shown in Fig.1 is a 2D conceptual design with its gradient in [T/m] versus its coil size represented by the equivalent coil width w_{eq} [3]. The hotspot temperature is fixed at ~350 K. For the designs with a 30 ms delay it is noticed that an increase of the time delay by 5 ms (30 to 35 ms) leads to a hotspot increase by ~50 K when the magnet is operated at nominal. With 50 mm aperture magnet, this study coupled to previous results [1] demonstrates that the 2-layers configuration becomes less efficient compare to 4-layers layouts at about w_{eq} = 33 mm [2] (vertical blue line in Fig. 1). This is due to a worse coil compaction coming from the large copper wedges in a 2 layer large cable magnet. The impact of a smaller protection delay by 10 ms allows for a strengthening of the gradient by ~20 T/m or a coil size reduction by ~13% at the baseline gradient of 360 T/m. To reach 360 T/m, a *perfect* design needs an

equivalent coil width of 26 mm (30 mm) for a protection time delay of 30 ms (40 ms), which could be translated for a 2-layers design in a cable width of 13 mm (15 mm). Actually, in that specific case, the cable has to be about 20% wider to accommodate the loss due its discrete nature – copper wedges and inter-layer insulation – leading to a cable width of 15.6 mm (18 mm).

C. Discussion

To select a design the windability of the cable through its number of strand and compaction shall be taken into account. So far, only Nb_3Sn quadrupoles with large aperture > 90 mm have been designed, manufactured and tested (TQ, HQ, LQ, QXF) and dipoles with small apertures < 60 mm (D20, HD series, 11T), for FCC MQ the combination of a small aperture and a quadrupole layout is challenging for the cable mechanical stabilility while winding. It turned out that the 11T and MQXF cables made of 40 strands "have been characterized by marginal mechanical stability" [7]. Based on these considerations, the cable width to reach 360 T/m and some additional design iterations (electromagnetic and protection), a cable made of 35 strands of 0.85 mm in diameter is selected.

III. 2 LAYER DESIGN

A. Cable design

The cable features are reported in Table I. Made of 0.85 mm strands, the first generation QXF cable with a 0.55° keystone angle and RRP strands is taken as a reference to estimate the MQ cable compaction. Therefore, a compaction of 15.4% is used for the thin edge of the MQ cable, a keystone angle of 0.4° helps to compact the thick edge (8.9%) in an attempt to improve the mechanical stability of the cable. With RRP strands the cable degradation shall not be an issue [8].

B. Electromagnetic design

Each aperture of the 2-in-1 FCC Main Quadrupole is based on the so-called cos-2θ coil layout (Fig. 2). The iron yoke is 600 mm in diameter and features the same holes for cryogenic purpose than the FCC MB [10],[11],[12]. The main characteristics of the FCC MQ are reported in Table II.

A field quality analysis taking into account the geometry of the coil, the saturation of the iron and the persistent current in the strand filaments is performed on the first two allowed harmonics b_6 and b_{10}. For the filament sizes, the state of the art with 55 µm and the FCC target with 20 µm, are investigated (Fig. 3). At low current b_6 reaches 23 units whereas b_{10} stays below 2 units.

An estimation of the random geometric errors is performed on the coils and leads to a RMS value σ_n for the n^{th}-harmonic [13]:

$$\sigma_n = d\alpha\beta^n$$

where d is the displacement from nominal in µm, $n > 2$ is the harmonic order, $\beta = 0.59$ and $\alpha = 0.4$ (or 0.8 for allowed harmonics: b_6 b_{10} b_{14} and so on [14]).

C. Protection analysis

The magnet is designed with a relatively tight time margin: 30 ms to 350 K. It means that the copper in the cable is sized such that the hotspot temperature does not exceed 350 K if the magnet quenches at 105% of the nominal current and the quench protection system (including quench detection, validation, switches, and the active protection heating system) is able to effectively quench the entire coil in 30 ms [15][16].

The magnet protection is based on the CLIQ (Coupling Loss Induced Quench) technology [17]. The CLIQ system relies on a charged capacitor bank to be discharged in the magnet windings upon the quench detection. The transport current oscillation and, therefore, magnetic field variation generate inter-filament and inter-strand coupling losses (Fig. 4), which rapidly quench the superconducting cables. The technology was developed over the past years at CERN within the HL-LHC project. Measurements and simulations have demonstrated more efficient performance than conventional quench protection heaters [18][19]. Actually CLIQ will be used in the HL-LHC inner triplet quadrupoles alongside with the protection heaters [18].

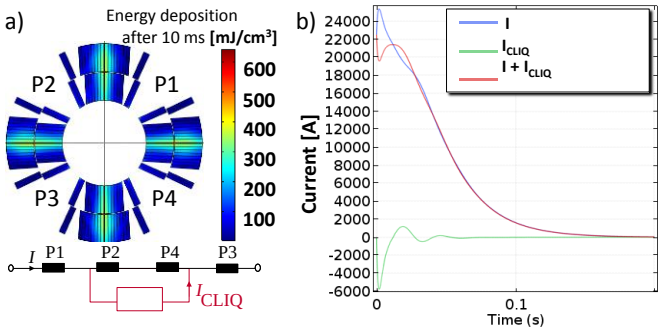

Fig. 4. a) CLIQ configuration and the simulated loss deposition in the preliminary protection analysis. b) Simulated currents after CLIQ discharge.

The protectability of the FCC main quadrupole is analyzed by assuming 21 ms time delay for the quench detection, validation and switch operation. The CLIQ system is connected across one half of each magnet aperture, as shown in Fig.4. The highest magnetic field change rate occurs at the coil mid-planes, thus most energy is deposited there. The present CLIQ unit has a capacitance of 50 mF, and it is charged to 500 V.

Simulation is performed using the recently released STEAM-SIGMA model builder and COMSOL FEM simulation [20][21][22]. The simulated energy deposition within the first 10 ms after CLIQ discharge is shown in Fig 4. The oscillations of the transport current in the coil sections after CLIQ discharge and the current decay due to resistance increase in the windings are reported in Fig. 4.

Based on the current decay profile the hotspot temperature is estimated analytically using the adiabatic MIITs concept [15] and the assumed 21 ms initial delay at constant current. At nominal current the hotspot temperature is about 300 K, and 350 K at 105% of the nominal current. The peak voltage to ground was 250 V and associated with half of the initial CLIQ discharge voltage. It is worth noticing that the protection at low current (1 kA) can be obtained with this CLIQ configuration even if the energy margin to quench is higher.

D. Collared mechanical structure

A collared structure similar to LHC MQ is numerically analyzed with the CEA in-house code: Cast3m [23]. The self-supporting collar structure allows for a single aperture simulation, but still needs to be better proven with Nb_3Sn coils [24]. The geometry is shown in Fig. 5 and represent one eight of the collared aperture of the magnet. The double pancake is glued including the 4 Nb_3Sn coil blocks, the 3 copper wedges and the interlayer insulation. The other contacts are sliding without separation. The material properties are reported in Table III. The collars are 27.7 mm wide and 19.2 mm at the narrow location of the 8.5 mm thick key and their inner radius is 59.3 mm – almost identical to the LHC MQ collars.

TABLE III
MATERIALS PROPERTIES

Materials	E[GPa] @ 293 K	E[GPa] @ 4.2 K	Integrated thermal contraction 293 K to 4.2 K [mm/m]
Nb_3Sn	30	33	3.4e-3**
Epoxy	5	8	6.0e-3
13RM19 steel	200*	210**	2.7e-3*
DISCUP copper	96***	96	3.3e-3

*:[25], **:[27], ***:[28]

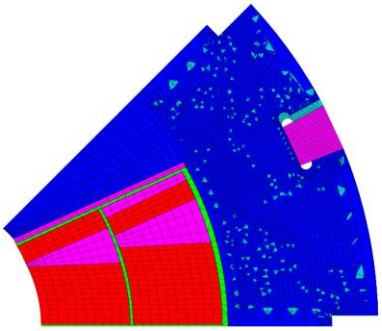

Fig. 5. FE mechanical model of one aperture eighth on Cast3m with smeared out material properties defined in Table III. A front collar with its nose and a back collar with a separated pole piece are simulated.

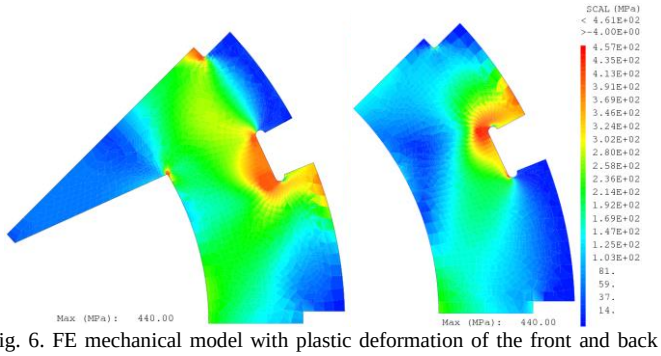

Fig. 6. FE mechanical model with plastic deformation of the front and back collars. The von Mises stress saturates at 440 MPa, the yield strength of the 13RM19 grade steel.

Four different steps are simulated in elastic mode: the collaring, the creep of 10% of the Nb_3Sn double pancake, the cool-down of the magnet and finally the energization of the coils.

TABLE IV
PEAK AND AVERAGE AZIMUTHAL STRESSES IN THE Nb_3Sn COIL BLOCKS

[MPa]	Collaring	+ Creep	+ Cool-down	+ Powering
Peak	-101.5	-91.4	-88.5	-111.1
Average	-85.5	-76.9	-73.2	-69.7

Under nominal powering the collaring provides a coil-pole minimal compression of 5 MPa. At each stage, the azimuthal peak stress and the average stress level in the coil blocks are recorded in Table IV. For the collar a plastic model is eventually implemented in which the stress in the collar saturates at 440 MPa according to the yield strength at 0.2% of the 13RM19 graded steel of LHC MQ collar [25] (see Fig. 6). This model leads to an increase of the peak stress by 10 MPa whereas the average stress remains the same. In any case, the level of stress is well below the 150 MPa limit for Nb_3Sn coil at room temperature and below the 125 MPa at which a strong creep behavior has been observed [26].

IV. CONCLUSION

An exploration of the 2-layers design options for the FCC Main Quadrupole has been carried out. The study is performed using the same assumptions for what concerns conductor and material properties as the FCC 16 T dipole development program. A gradient of 360 T/m is found providing a good balance between performance and complexity of the magnet technology. At this stage, a design with a 35-strand cable slightly narrower than the High Luminosity MQXF cable is selected as baseline. The magnet design meets the field quality target requirements and can be mechanically constrained by a conventional collar structure with an azimuthal peak stress value slightly above 110 MPa in the Nb_3Sn during collaring. The protection investigation shows that a single CLIQ unit (50 mF and 500 V) allows for a protection of the magnet within the 350 K hotspot limit.

As a next step, the windability of the cable shall be carefully investigated. Some tests are already foreseen in the framework of a collaboration agreement between CERN and CEA.

ACKNOWLEDGMENT

The authors would like to thank Susana Izquierdo Bermudez (CERN), Ian Pong (LBNL), Marco Prioli (CERN), Felix Wolf (CERN), for useful discussion about field quality, cable dimension, magnet protection and Nb_3Sn coil mechanical creep.

REFERENCES

[1] C. Lorin, D. Simon, H. Felice, J-M Rifflet, D. Schoerling “Design of a Nb3Sn 400 T/m quadrupole for the Future Circular Collider”, IEEE Transactions on Applied Superconductivity,4004905, 2018.

[2] C. Lorin, "FCC Main Quadrupoles", 4th FCC week, 9-13 April 2018, Amsterdam, the Nederlands, [Online]. Available: https://indico.cern.ch/event/656491/contributions/2920307/

[3] L. Rossi and E. Todesco, "Electromagnetic design of superconducting quadrupoles" Physical Review: Special Topics Accelerator and Beams, 102401, 2006.

[4] F. Savary et al., "Design and construction of the full-length prototype of the 11 T dipole magnet for the High Luminosity LHC project at CERN", IEEE Transactions on Applied Superconductivity, 4007106, 2018.

[5] D. W. Cheng et al. "Fabrication and assembly performance of the first 4.2 m MQXFA magnet and mechanical model for the Hi-Lumi HC upgrade" IEEE Transactions on Applied Superconductivity 4006207, 2018.

[6] F. Lackner et al., "Fabrication of the 7.3 m long coils for the prototype of MQXFB, the Nb_3Sn low-b quadrupole magnet for the HiLumi LHC", IEEE Transactions on Applied Superconductivity 4005605, 2018.

[7] G. Ambrosio, "Nb_3Sn high field magnets for the High Luminosity LHC upgrade project", IEEE Transactions on Applied Superconductivity, 4002107, (2015).

[8] J. Fleiter et al., "Optimization of Nb3Sn Rutherford cables geometry for the high-luminosity LHC", IEEE Transactions on Applied Superconductivity, 4004305, (2017).

[9] T. Salmi, M. Prioli, "Magnet quench protection", EuroCirCol Annual meeting, Karlsruhe Institut of Technology, 17 October 2018. https://indico.cern.ch/event/733292/contributions/3147632/

[10] B. Caiffi et al., "3D mechanical design of EuroCirCol cosθ 16 T bending dipole", to be published in IEEE Transactions on Applied Superconductivity, (2019).

[11] C. Pes et al, "Magnetic and Mechanical Design of the Block-Coil Dipole Option for the Future Circular Collider", to be published in IEEE Transactions on Applied Superconductivity, (2019).

[12] F. Toral, J. Munilla, T. Salmi, "Magnetic and Mechanical Design of a 16 T Common-coil Dipole for an FCC", IEEE Transactions on Applied Superconductivity, 4004305, (2018).

[13] P. Ferracin, W. Scandale, E. Todesco, R. Wolf, "Modelling of random geometric errors in superconducting magnets with applications to the CERN Large Hadron Collider" Physical Review: Special Topics Accelerator and Beams, 122403, (2000)

[14] S. Izquierdo-Bermudez, Private communication, 9 july 2018

[15] E. Todesco, in Proceedings of WAMSDO: Workshop on accelerator magnet superconductors, design and optimization, edited by E. Todesco, CERN-2013-006 (CERN, Geneva, 2013), pp. 10–16.

[16] T. Salmi, et al., "Quench protection analysis integrated in the design of dipoles for the Future Circular Collider", Physical Review Accelerators and Beams 20 3, 032401, 2017

[17] E. Ravaioli, CLIQ: A new quench protection technology for superconducting magnets, Ph.D. thesis, University Twente and CERN, 2015

[18] E. Ravaioli et al., "Quench Protection Performance Measurements in the First MQXF Magnet Models", IEEE Trans.Appl.Supercond. 28 3, 4701606, 2018

[19] T.Salmi, et al., "Quench protection of the 16 T Nb3Sn dipole magnets designed for the Future Circular Collider" ,To be presented at ASC 2018

[20] STEAM website: http://cern.ch/steam (accessed 15.10.2018)

[21] STEAM team. SIGMA documentation v1.0. Tech. rep. EDMS 2021390. Geneva: CERN, 2018

[22] L. Bortot, et al., "STEAM: A Hierarchical Cosimulation Framework for Superconducting Accelerator Magnet Circuits", IEEE Trans.Appl.Supercond. 28 3, 4900706, 2018

[23] P. Verpaux, T. Charras, and A. Millard, "CASTEM 2000 une approche moderne du calcul des structures" in Calcul des structures et intelligence artificielle, Pluralis, pp. 261-271, (1988)

[24] S. Feher et al., "Development and Test of LARP Technological Quadrupole (TQC) Magnet", IEEE Trans.Appl.Supercond. 17,2,June 2007

[25] C. Lanza, D. Perini, "Characteristics of the austenitic steels used in the LHC Main dipoles", LHC Project Report 537, (2001)

[26] F. Wolf, F. Lackner, C. Scheuerlein, D. Schoerling, D. Tommasini, "Effect of transverse stress applied during reaction heat treatment on the stiffness of Nb_3Sn Rutherford cable stacks", Poster at the 4th FCC Week in Amsterdam, 9-13 April 2018, https://indico.cern.ch/event/656491/contributions/2939088/

[27] D. Tommasini et al., "Baseline parameters of the 16 T dipoles for the FCC", https://indico.cern.ch/event/556692/contributions/2591664/ Presentation at the 3rd FCC Week in Berlin, 29 May – 2 June, 2017

[28] C. Scheuerlein et al, "Mechanical properties of the HL-LHC 11 T Nb3Sn magnet constituent materials", IEEE Transactions on Applied Superconductivity, 4003007, (2017)